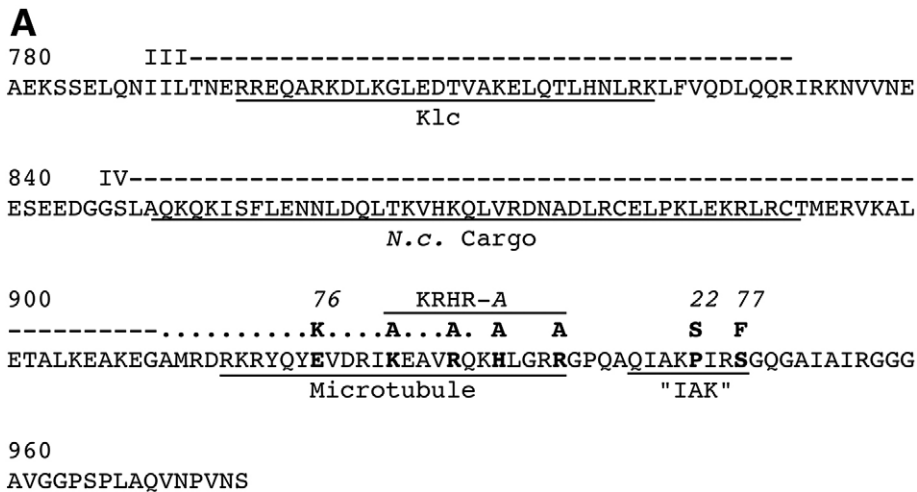**CORRECTION**

Kinesin-1 tail autoregulation and microtubule-binding regions function in saltatory transport but not ooplasmic streaming

Pangkong Moua, Donna Fullerton, Laura R. Serbus, Rahul Warrior and William M. Saxton

There was an error published in Development **138**, 1087-1092.

A *Drosophila* fly strain was described as having a transgene (Khc^{4R-A}) with mutations that produce Khc protein with four basic amino acids in the tail microtubule-binding domain changed to alanine (Fig. 1A, Fig. 4B). The identities of two of the amino acids that were changed were misreported. The correct amino acid changes are K925A (not R923A), R929A, H932A (not R935A) and R936A. Accordingly, the allele has been renamed Khc^{KRHR-A}. A revised Fig. 1A is provided below.

This error does not affect the conclusions of the paper. The authors apologise to readers for this mistake.

```
A
780      III-----------------------------------------
AEKSSELQNIILTNERREQARKDLKGLEDTVAKELQTLHNLRKLFVQDLQQRIRKNVVNE
                            Klc

840      IV------------------------------------------------
ESEEDGGSLAQKQKISFLENNLDQLTKVHKQLVRDNADLRCELPKLEKRLRCTMERVKAL
                        N.c. Cargo

900                      76    KRHR-A              22 77
----------...........K....A...A. A    A        S  F
ETALKEAKEGAMRDRKRYQYEVDRIKEAVRQKHLGRRGPQAQIAKPIRSGQGAIAIRGGG
                Microtubule                    "IAK"

960
AVGGPSPLAQVNPVNS
```

Kinesin-1 tail autoregulation and microtubule-binding regions function in saltatory transport but not ooplasmic streaming

Pangkong Moua[1,*], Donna Fullerton[2], Laura R. Serbus[2], Rahul Warrior[3] and William M. Saxton[1,2,†]

SUMMARY

The N-terminal head domain of kinesin heavy chain (Khc) is well known for generating force for transport along microtubules in cytoplasmic organization processes during metazoan development, but the functions of the C-terminal tail are not clear. To address this, we studied the effects of tail mutations on mitochondria transport, determinant mRNA localization and cytoplasmic streaming in *Drosophila*. Our results show that two biochemically defined elements of the tail – the ATP-independent microtubule-binding sequence and the IAK autoinhibitory motif – are essential for development and viability. Both elements have positive functions in the axonal transport of mitochondria and determinant mRNA localization in oocytes, processes that are accomplished by biased saltatory movement of individual cargoes. Surprisingly, there were no indications that the IAK autoinhibitory motif acts as a general downregulator of Kinesin-1 in those processes. Time-lapse imaging indicated that neither tail region is needed for fast cytoplasmic streaming in oocytes, which is a non-saltatory bulk transport process driven solely by Kinesin-1. Thus, the Khc tail is not constitutively required for Kinesin-1 activation, force transduction or linkage to cargo. It might instead be crucial for more subtle elements of motor control and coordination in the stop-and-go movements of biased saltatory transport.

KEY WORDS: *Drosophila*, Kinesin-1, Tail, Mitochondria transport, mRNA localization, Streaming

INTRODUCTION

In large cells, such as oocytes and neurons, normal development and function require asymmetric movement and localization of cytoplasmic components by molecular motor proteins. In vitro studies have led to a deep understanding of force generation by the mechanochemical head domain of Kinesin-1 (Brady, 1985; Vale et al., 1985; Valentine and Gilbert, 2007). By contrast, our understanding of the non-mechanochemical elements of Kinesin-1 that define how it works in vivo is incomplete (Adio et al., 2006; Hirokawa and Takemura, 2005; Rice and Gelfand, 2006).

Metazoan Kinesin-1 comprises two elongated heavy chains (Khcs) and two light chains (e.g. Klcs). Khc dimerizes to form a flexible coiled-coil stalk region with N-terminal head domains at one end and small globular tail domains at the other. Light chains attach near the C-terminal end of the stalk. To generate processive motion toward microtubule plus-ends, the two heads alternate in cycles of ATP hydrolysis and microtubule binding/release (Vale and Milligan, 2000; Valentine and Gilbert, 2007). In vitro testing has shown that residues in the conserved tail IAK motif (QIAKPIRS in *Drosophila*) can interact with the head to hinder ADP release, weaken head-microtubule interaction and downregulate processive movement (Cai et al., 2007; Coy et al.,

1999; Dietrich et al., 2008; Friedman and Vale, 1999; Hackney et al., 2009; Hackney and Stock, 2000; Stock et al., 1999; Wong et al., 2009; Yonekura et al., 2006). These and other results have led to a classic hypothesis for Kinesin-1 function: the stalk of a cargo-free motor folds such that the IAK region interacts with and inhibits force generation by the head, then cargo binding via Klcs or analogous linkers activates force generation and movement along microtubules by extending the stalk and relieving IAK-head repression (for a review, see Gindhart, 2006; Rice and Gelfand, 2006; Verhey and Rapoport, 2001). Additional studies indicate that folded inactive Kinesin-1 may remain associated with both cargo and microtubules via an ATP-independent microtubule-binding region in the tail, perhaps to help keep motor-cargo complexes poised to move (Dietrich et al., 2008; Hackney et al., 2009; Hackney and Stock, 2000; Navone et al., 1992; Seeger and Rice, 2010).

How the IAK and microtubule-binding elements of the Khc tail contribute to development and to specific Kinesin-1-driven transport processes in metazoans is not clear. To address this, we identified missense mutations in the tail-coding region of *Drosophila Khc* and studied their effects. We found that normal IAK and tail microtubule-binding regions have equivalent positive influences on saltatory transport processes and that neither is needed for bulk ooplasmic streaming. This suggests that the IAK is not a general repressor of Kinesin-1-driven transport in vivo and that saltatory mechanisms have critical complexities that demand regulatory control by the Khc tail.

MATERIALS AND METHODS
Generation of *Khc* mutations
Recessive *Khc* mutations generated with ethyl methane sulfonate were identified via F2 lethal screens (Brendza et al., 1999; Lei and Warrior, 2000; Liu et al., 1999; Saxton et al., 1991).

[1]Department of Biology, Indiana University, Bloomington, IN 47405, USA.
[2]Department of Molecular Cell and Developmental Biology, University of California, Santa Cruz, CA 95064, USA. [3]Department of Developmental and Cell Biology, University of California, Irvine, CA 92697, USA.

*Present address: Department of Cell and Molecular Biology, Northwestern University, Chicago, IL 60611, USA
†Author for correspondence (bsaxton@ucsc.edu)

Analysis of mitochondria transport and ooplasmic streaming and in situ hybridization

GFP-mitochondria (mitoGFP) transport assays were performed as described (Barkus et al., 2008; Pilling et al., 2006). Preparation of mutant female germline clones, streaming analyses and *oskar* (*osk*) mRNA fluorescent in situ hybridization were performed as described (Cha et al., 2002; Serbus et al., 2005).

Fluorescence imaging

Nerves and axon terminals were imaged by confocal fluorescence microscopy in dissected, fixed, immunostained larvae (Barkus et al., 2008; Hurd and Saxton, 1996). Primary antibodies were mouse anti-Cysteine string protein (CSP; 1:500), mouse anti-Fasciclin II (1:350) and rabbit anti-*Drosophila* Khc (1:500, Cytoskeleton). Secondary antibodies were goat anti-mouse or anti-rabbit Alexa Fluor 594 (1:1000, Molecular Probes) and goat anti-mouse Cy5 (1:1000, Southern Biotech). Imaging was performed with a BioRad MRC600 or Leica SP5 confocal microscope system. Fluorescence was quantified in boutons and oocytes using ImageJ by measuring average pixel intensities in regions of interest that were outlined by intensity thresholding. Background fluorescence from adjacent muscle cells was subtracted from Khc intensity values in boutons.

Time-lapse imaging

Time-lapse imaging of mitochondria transport was performed with intact larvae using a spinning disk confocal microscope (Perkin-Elmer Ultraview). Larvae were anesthetized with desflurane (Baxter) in a sealed imaging chamber (Fuger et al., 2007). After imaging, larvae were returned to culture and data were analyzed only from larvae that survived for at least another 24 hours.

Statistical analyses

All statistical comparisons were performed by two-tailed *t*-tests with unequal variance, except where otherwise noted.

RESULTS AND DISCUSSION

To identify residues in the Khc tail that are crucial in development, randomly generated lethal *Khc* alleles were sequenced. Missense mutations were identified in the conserved IAK motif (Khc^{22}, P945S; Khc^{77}, S948F) and in the ATP-independent tail microtubule-binding region (Khc^{76}, E920K) (Fig. 1A). Lethal phase and complementation tests of the tail alleles with other *Khc* alleles indicated that they are recessive and hypomorphic (partial loss of function). Two well-known hypomorphic head alleles known to impair Khc mechanochemistry (Khc^{23}, E164K; Khc^{17}, S246F) (Brendza et al., 1999) were used for comparison. Comparison by lethal complementation indicated that Khc^{77} and Khc^{23} are the most severe and Khc^{76} is the least severe of the five alleles. All five alleles, when combined with nulls, caused classic larval posterior paralysis and focal accumulation of synaptic proteins in axons (Fig. 1B), indicating distal neuropathy caused by defective axonal transport (Gho et al., 1992; Hurd and Saxton, 1996; Pilling et al., 2006; Reid et al., 2002).

IAK mutations in *Neurospora* Khc inhibit growth and cause a dramatic 40-fold increase in Khc concentration at hyphae tips, suggesting overactive, cargo-free Kinesin-1 movement towards microtubule plus-ends (Seiler et al., 2000). To determine whether mutations in the *Drosophila* IAK motif have similar effects, we compared the distributions of Khc, mitochondria and Fasciclin in motor axon terminals, towards which plus-ends are oriented (Stone et al., 2008). Combining the most severe IAK allele, Khc^{77}, with a null allele (Khc^{27}) resulted in dystrophic terminals with few boutons and few mitochondria (Fig. 1C). Quantification of anti-Khc intensity per unit area in single optical sections of individual boutons indicated no significant difference between wild type and $Khc^{77/27}$ (wild type: 62.3±27.0 intensity units/pixel ± s.e.m., 26
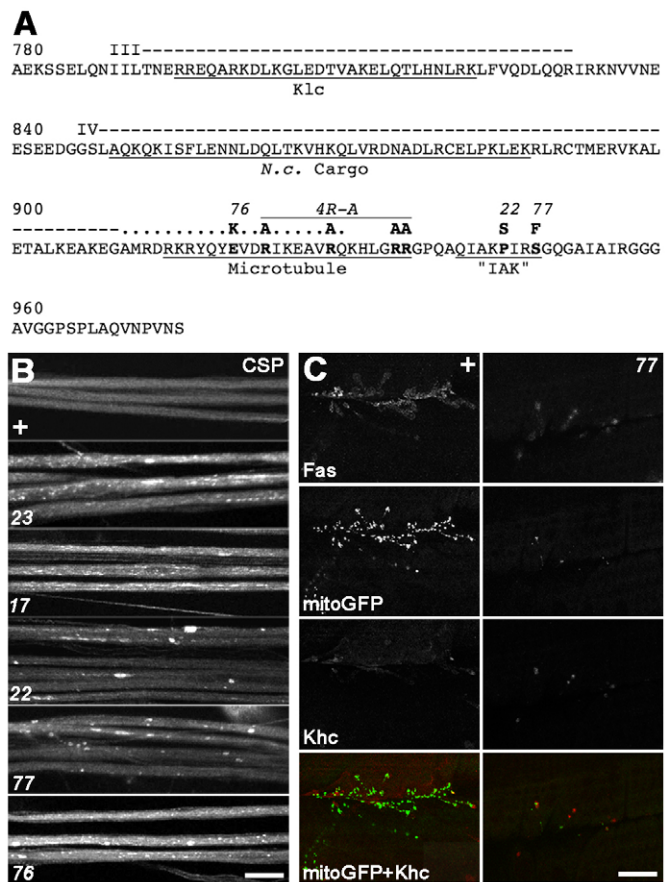

Fig. 1. *Khc* tail mutations inhibit Kinesin-1-driven axonal transport. (**A**) Locations of missense mutations in the Khc tail. The sequence of the C-terminal region of *Drosophila* Khc (codons 780-975) is shown with changes caused by the tail alleles (Khc^{76}, Khc^{22}, Khc^{77}, 4R-A) noted above. Coil 3 of the stalk (III, dashed line) includes binding sites for Klc, Milton and their associated cargoes (Klc). Coil 4a-b (IV, dashed line) includes a cargo binding site in *Neurospora* (N.c. Cargo). Coil 4c (dotted line) includes part of a tail microtubule-binding region (Microtubule) that extends towards a conserved IAK motif ("IAK") that can interact with the N-terminal Khc head to inhibit force generation. (**B**) Fluorescence images of nerves in third instar larvae stained with anti-CSP. Images are representative of 10-15 larvae per genotype, either wild type (+) or the indicated *Khc* allele over the Khc^{27} null allele. (**C**) z-projections of axon terminals on muscles 6/7 in segment A3 of control (+) and Khc^{77}/Khc^{27} (77) mutant larvae. Larvae expressing mitochondria-targeted GFP (mitoGFP) in neurons (green in merge) were stained for Khc (red in merge) and Fasciclin (Fas). Scale bars: 30 μm in B; 20 μm in C.

boutons, 6 larvae; $Khc^{77/27}$: 73.2±18.0, 6 larvae, 14 boutons; *P*<0.74). Thus, although IAK alleles reduce terminal growth, they do not cause a *Neurospora*-like 40-fold increase in Khc concentration at microtubule plus-ends. This suggests that our mutations in the *Drosophila* IAK autoinhibition motif do not overactivate Kinesin-1 in axons.
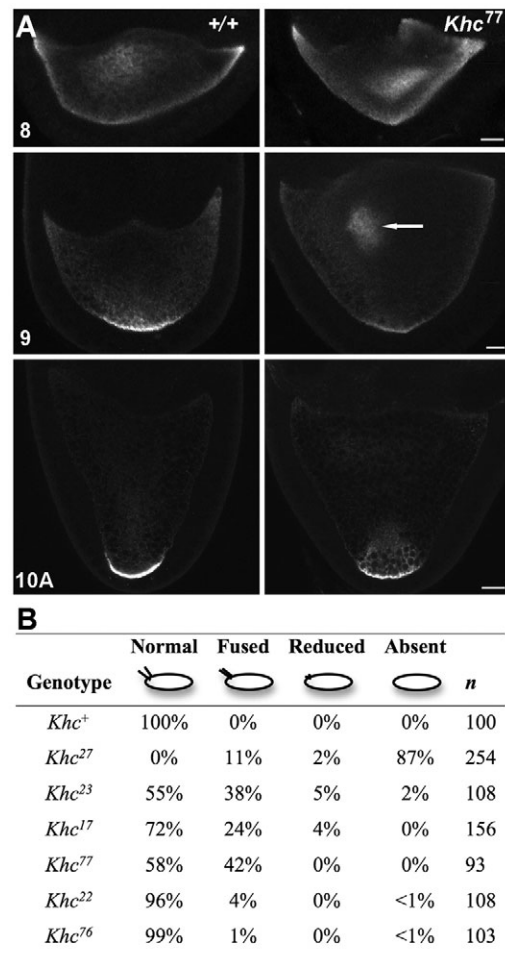
To test the effects of tail mutations more directly, larvae with mitochondria-targeted GFP (mitoGFP) expressed in neurons were anesthetized and mitochondria in segmental nerve axons were imaged through the ventral body wall (see Movies 1-3 in the supplementary material). The IAK alleles (Khc^{77}, Khc^{22}), the tail microtubule-binding site allele (Khc^{76}) and the two *Khc* head alleles (Khc^{23}, Khc^{17}) all inhibited both anterograde and retrograde flux of
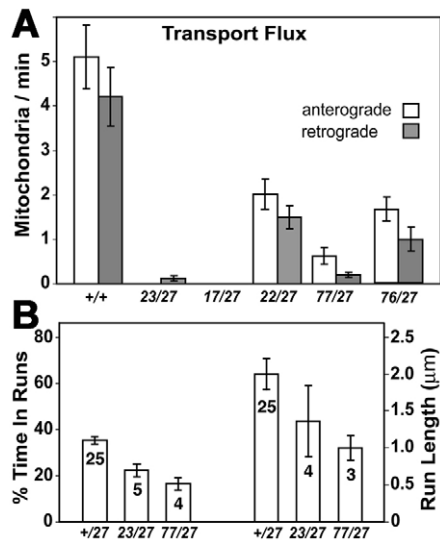
Fig. 2. *Khc* IAK motif mutations inhibit axonal transport of mitochondria. *Drosophila* larvae of the indicated *Khc* genotypes expressing mitoGFP in neurons were anesthetized and segmental nerves imaged by time-lapse confocal microscopy (see Movies 1-3 in the supplementary material). (**A**) The number of mitochondria per minute that moved anterograde or retrograde (flux) into a photobleached zone in one segmental nerve per larva was counted for ten animals per genotype (mean ± s.e.m.). All mutant means were significantly lower than that of wild type ($P<0.05$). (**B**) The percentage of time that anterograde-moving mitochondria spent in anterograde runs relative to total tracking time, which included pauses and reverse runs, is on the left. Mean anterograde run lengths are on the right. Values were determined by digital tracking in five larvae per genotype (mean ± s.e.m.). Sample size (number of mitochondria tracked) is noted in each bar.

Fig. 3. *Khc* IAK motif mutations inhibit body axis patterning in oocytes. (**A**) Fluorescent in situ hybridization images for *osk* mRNA in wild-type (left) and *Khc^77* mutant (right) *Drosophila* oocytes at the indicated stages of oogenesis. The arrow indicates a lagging central concentration of *osk* in stage-9 mutants. Scale bars: 25 μm in stage 8; 50 μm in stages 9 and 10A. (**B**) Eggs from female germline clones homozygous for the *Khc* alleles indicated on the left were scored for defects in dorsal appendage morphology that indicate defective dorsal-ventral patterning.

axonal mitochondria (Fig. 2A). Such bidirectional inhibition is consistent with studies that indicate a dependence of Dynein, the retrograde mitochondria motor, on Khc (Brady et al., 1990; Ling et al., 2004; Martin et al., 1999; Pilling et al., 2006). Anterograde motions of the few mitochondria that did move in larvae mutant for the more severe tail and head alleles were tracked and analyzed. Mean run velocities (aggregated by mitochondrion) were: wild type, 0.56±0.02 μm/second (25 mitochondria); *Khc^23*, 0.82±0.09 μm/second (4 mitochondria); and *Khc^77*, 0.70±0.11 μm/second (3 mitochondria). The mean for *Khc^77* did not differ from that of wild type ($P<0.6$) or *Khc^23* ($P<0.17$). In both mutants, the percentage of time that moving mitochondria spent in anterograde runs was less than for wild type ($P<0.003$), but the percentage run times for head and IAK mutants did not differ from each other ($P<0.11$) (Fig. 2B). Mean anterograde run length for *Khc^77* was less than for wild type ($P<0.001$), but again head and IAK mutants were not different ($P<0.26$). In summary, these tests revealed no substantial differences in transport defects caused by tail IAK mutations and by mutations that reduce Khc activity by impairing head mechanochemistry. This suggests that the normal function of the Khc IAK motif during the axonal transport of mitochondria is to facilitate, rather than downregulate, Kinesin-1-driven cargo transport.
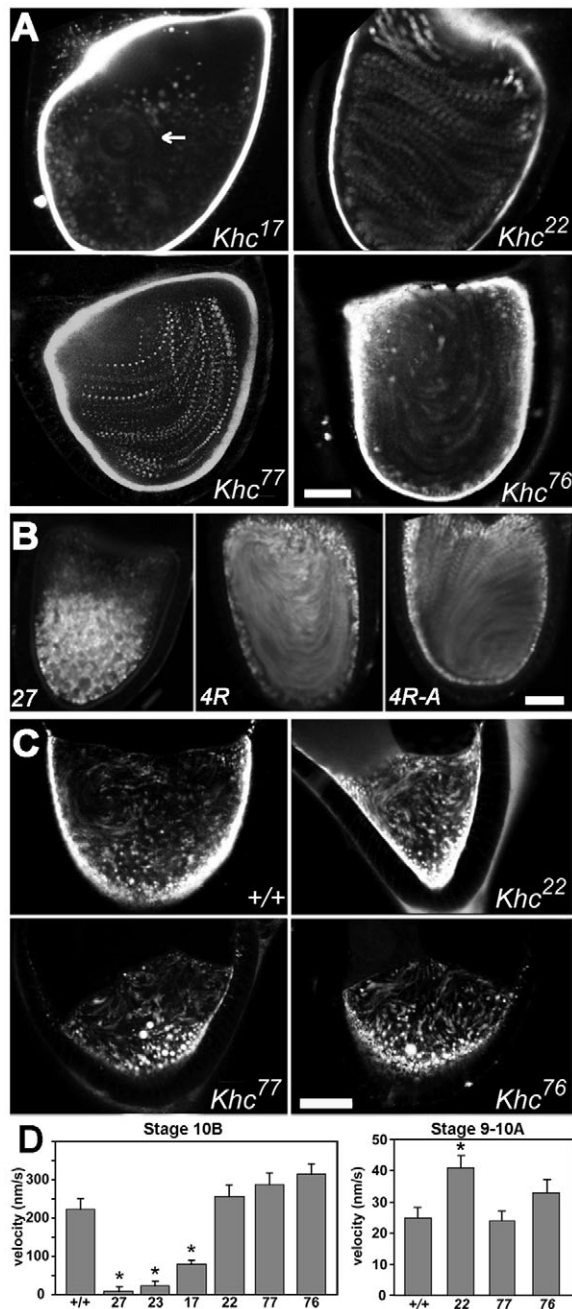
To test other Kinesin-1-dependent processes, we turned to oogenesis. Khc is required in *Drosophila* oocytes for proper localization of some key developmental polarity determinants (Brendza et al., 2000; Brendza et al., 2002; Cha et al., 2002; Duncan and Warrior, 2002; Januschke et al., 2002; Palacios and St

Johnston, 2002; Zimyanin et al., 2008). To test the effects of IAK alleles, fluorescent in situ hybridization was used to examine the localization of *osk* mRNA, a posterior determinant, in mutant oocytes (Fig. 3A). Normally, *osk* shifts from a diffuse cortical distribution towards the oocyte center in stage 8 and then concentrates at the posterior cortex. Mutant stage-9 oocytes showed a lagging central concentration (12 of 14 *Khc^77* and 6 of 9 *Khc^22* versus 2 of 26 wild type) and an apparent weak concentration of *osk* at the posterior. Fluorescence quantification at the posterior of *Khc^77* and wild-type oocytes processed in parallel showed 89±7 ($n=14$ oocytes) and 115±6 ($n=9$) intensity units/pixel, respectively, whereas *Khc^22* and its parallel control showed 101±9 ($n=7$) and 136±2 ($n=13$), respectively. Both mutant means were significantly lower than that of wild type ($P<0.01$). The aberrant stage-9 central concentration and the weak stage-10A posterior accumulation are comparable to the effects of the *Khc^17* and *Khc^23* head alleles (Serbus et al., 2005; Zimyanin et al., 2008).

DEVELOPMENT

Fig. 4. IAK and tail microtubule-binding mutations do not inhibit Khc-dependent ooplasmic streaming. (**A**) Fluorescent yolk endosomes were imaged by time-lapse microscopy in stage-10B *Drosophila* oocytes homozygous for the indicated *Khc* alleles. Panels show time projections of 15 frames each (225 seconds total). Moving endosomes appear in the projections as streaks or trails of spots. The arrow indicates a residual circular area of streaming in a *Khc*[17] head mutant oocyte (compare Movies 4 and 5 in the supplementary material). By contrast, streaming appeared normal in tail mutants (compare Movies 4 and 6 in the supplementary material). (**B**) Time projections of oocytes homozygous for a *Khc* null allele without any *Khc* transgene (*27*), with a wild-type *Khc* transgene (*4R*), or with a mutant *Khc* transgene that has four arginine codons converted to alanines in the tail microtubule-binding region (*4R-A*). Streaming patterns were normal in the *4R-A* mutant. (**C**) Time projections of slow streaming in stage-9 oocytes homozygous for the indicated tail alleles. Motion appeared normal in the mutants. Scale bars: 40 µm. (**D**) Mean velocities (+ s.e.m.) of moving yolk endosomes in stage-10B and stage-9 oocytes homozygous for the Khc alleles indicated on the *x*-axis. Ten randomly selected yolk endosomes were tracked in each of five oocytes per genotype. Sample sizes were 45-50 moving endosomes. Asterisks indicate values significantly different from the wild type as determined by general linear modeling (*P*<0.05).

Khc null alleles reduce localization of the dorsal determinant *gurken* (*grk*) mRNA to the anterior lateral cortex during stages 7-9 (Brendza et al., 2002; Duncan and Warrior, 2002; Januschke et al., 2002), suppressing dorsal-ventral (DV) pattern formation and subsequent development of normal dorsal appendages on the egg chorion (Fig. 3B). To test the influence of tail alleles on DV patterning, we compared dorsal appendage configurations on eggs from homozygous null, head mutant and tail mutant germline clones. The most severe head and IAK hypomorphic alleles, *Khc*[23] and *Khc*[77], inhibited dorsal appendage formation on ~45% of the eggs produced from homozygous mutant germline clones (Fig. 3B), consistent with defective Grk dynamics and DV patterning. Although it is not well understood how Kinesin-1 contributes to DV patterning, these results are consistent with a positive role for the wild-type IAK motif in axis determination.

Our studies show that IAK motif mutations inhibit rather than overactivate Kinesin-1-dependent transport processes. This suggests that, despite the autoinhibitory effects of the IAK motif on Khc mechanochemistry in vitro, it is not a global repressor of Kinesin-1-driven cargo transport in vivo. One caveat is that the two IAK alleles we analyzed may both enhance rather than disrupt tail-head autoinhibitory interactions and that a true disruption of autoinhibition would be dominant or at least cause phenotypes qualitatively different from null and hypomorphic mutations. Arguing against this is the fact that mutations in the *Neurospora* IAK motif that have been proven to overactivate mechanochemistry in vitro actually cause loss-of-function growth phenotypes similar to those caused by a null (Seiler et al., 2000). In addition, a mutation that overactivates a *C. elegans* Kinesin-2 (OSM-3) in vitro by inhibiting stalk folding and tail-head interaction causes recessive loss-of-function phenotypes in vivo (Imanishi et al., 2006; Snow et al., 2004). These observations are consistent with the conclusion that, in multiple processes, defects that should disrupt tail-head autoinhibitory dynamics actually reduce rather than overactivate cargo transport.

In contrast to the saltatory single cargo localization processes discussed above, Kinesin-1-driven ooplasmic streaming in *Drosophila* generates bulk, non-saltatory cytoplasmic flows that facilitate mixing of ooplasm (Gutzeit and Koppa, 1982; Palacios and St Johnston, 2002). Flows during stages 7-10A, when much of the determinant localization is being accomplished, are disordered and slow. Then, in stage 10B, flows become global, well-ordered and fast. Interestingly, a premature transition from slow to fast streaming can be induced by injecting oocytes with inhibitory Dynein antibodies, suggesting that Dynein antagonizes Kinesin-1 to help suppress fast streaming during determinant localization (Serbus et al., 2005). This antagonistic motor relationship is unusual because in other transport processes that have been examined in detail, different microtubule motors alternate in a coordinated fashion with no direct antagonism (Gross et al., 2002; Ou et al., 2005; Welte, 2004).

To test for unique IAK influences on fast streaming, yolk endosome motion was analyzed. In stage 10B, the *Khc*[23] and *Khc*[17] head alleles allowed isolated areas of low-velocity

streaming, suggesting weak plus-end-directed force production (Fig. 4A and see Movies 4 and 5 in the supplementary material), consistent with defective head mechanochemistry (Serbus et al., 2005). Surprisingly, the Khc^{77} and Khc^{22} IAK alleles allowed robust ordered movement at high velocities (Fig. 4A and see Movies 4 and 6 in the supplementary material). This contrast between the effects of IAK and head alleles in fast streaming shows for the first time a clear separation in function for the tail and motor domains.

To determine whether the insensitivity of fast streaming to tail defects is unique to the IAK motif, we examined the effects of other tail mutations. Adjacent to the IAK is a region rich in positively charged residues that binds to microtubules in vitro, perhaps via electrostatic interactions (Seeger and Rice, 2010). The Khc^{76} allele, which alters this region, inhibited axonal transport (Fig. 1B and Fig. 2A) but, like the IAK alleles, supported robust fast streaming (Fig. 4A). To test the possibility that this was simply due to the mild nature of Khc^{76}, we created a transgenic allele (Khc^{4R-A}) in which four positively charged arginines in the tail microtubule-binding region were switched to neutral alanines (Fig. 1A) (generous gift from V. Gelfand and H. Kim, Northwestern University, IL, USA). In an otherwise Khc null background $\{Khc^{27}/Df(2R)Jp6; p[w^+ Khc^{4R-A}]/+\}$, the $4R-A$ mutation caused 50% lethality before the end of the third instar and axonal mitochondria flux was reduced ~30-fold (anterograde, 0.16± 0.10/minute; retrograde, 0.14±0.06/minute; n=7 larvae). These results confirm that the Khc^{4R-A} allele is severe, providing substantially less Khc function than the other tail alleles. Remarkably, one copy of the transgene fully rescued fast streaming in a Khc null background (15 of 15 oocytes examined; Fig. 4B). This indicates that, like the IAK residues tested, the Khc tail microtubule-binding region is not crucial for robust Kinesin-1 transport activity during fast ooplasmic streaming. Thus, despite the unique behaviors of the normal IAK and tail microtubule-binding regions in vitro, with respective negative and positive influences on Khc transport activity, their influences in the processes that we have tested do not differ: both parts of the tail facilitate mitochondria transport and mRNA localization and neither is required for fast ooplasmic streaming.

It is interesting to consider similarities and differences between the mechanisms of streaming and the other processes tested. Mitochondria transport in axons entails intermittent bursts of coordinated Kinesin-1 and Dynein activity to accomplish biased saltatory movement along well-ordered microtubules. The transport of osk and grk messenger ribonucleoprotein particles (mRNPs) is not so well understood, but Dynein and Kinesin-1 are both active during mid-late oogenesis and time-lapse imaging shows that fluorescence-tagged mRNPs move in a biased saltatory fashion (MacDougall et al., 2003; Zimyanin et al., 2008). In both processes, transport appears to be intermittent, so Kinesin-1 coordination with other motors might be important. Fast streaming is not saltatory, but rather entails persistent plus-end transport driven solely by Kinesin-1 along ordered cortical microtubules (Palacios and St Johnston, 2002; Serbus et al., 2005; Theurkauf et al., 1992). Perhaps the simplicity of persistent Kinesin-1 force generation in fast streaming makes modulation by the IAK and microtubule-binding regions dispensable.

To test the possibility that the IAK and microtubule-binding sequences influence streaming when Dynein and Kinesin-1 are both active, yolk endosome movements were studied in stage 8-9 oocytes. The Khc^{23} and Khc^{17} head alleles are known to substantially inhibit the velocity of slow streaming (Serbus et al.,

2005). Our tail alleles did not inhibit slow streaming; rather, yolk particles appeared to move somewhat faster. Quantification revealed that Khc^{22} oocytes had a 1.5-fold faster mean velocity than wild-type oocytes (Fig. 4C,D; $P<0.05$), an increase that suggests that the tail might help Dynein restrain ordered Kinesin-1 force generation during slow streaming. More extensive testing of Khc^{22} and other tail alleles will be required to determine whether this interpretation is valid. If so, it will support the hypothesis that the IAK motif significantly represses Kinesin-1 cargo transport activity in some situations.

We conclude that the IAK motif does not act as a general negative regulator of Kinesin-1 in the processes that we tested, with the possible exception of streaming. In the more common saltatory transport mechanisms that bias single cargo movement along microtubules towards discrete destinations, the IAK and the adjacent tail microtubule-binding sequences both make positive contributions. Whether they contribute to the tethering of motor-cargo complexes to microtubules and thus to processive motion, to the coordination of different types of microtubule motors, or to some as yet unidentified facet of saltatory transport mechanisms will be important questions to pursue in the future.

Competing interests statement
The authors declare no competing financial interests.

Supplementary material
Supplementary material for this article is available at
http://dev.biologists.org/lookup/suppl/doi:10.1242/dev.048645/-/DC1

References
Adio, S., Reth, J., Bathe, F. and Woehlke, G. (2006). Review: regulation mechanisms of Kinesin-1. *J. Muscle Res. Cell Motil.* **27**, 153-160.

Barkus, R. V., Klyachko, O., Horiuchi, D., Dickson, B. J. and Saxton, W. M. (2008). Identification of an axonal kinesin-3 motor for fast anterograde vesicle transport that facilitates retrograde transport of neuropeptides. *Mol. Biol. Cell* **19**, 274-283.

Brady, S. T. (1985). A novel brain ATPase with properties expected for the fast axonal transport motor. *Nature* **317**, 73-75.

Brady, S. T., Pfister, K. K. and Bloom, G. S. (1990). A monoclonal antibody against kinesin inhibits both anterograde and retrograde fast axonal transport in squid axoplasm. *Proc. Natl. Acad. Sci. USA* **87**, 1061-1065.

Brendza, K. M., Rose, D. J., Gilbert, S. P. and Saxton, W. M. (1999). Lethal kinesin mutations reveal amino acids important for ATPase activation and structural coupling. *J. Biol. Chem.* **274**, 31506-31514.

Brendza, R. P., Serbus, L. R., Duffy, J. B. and Saxton, W. M. (2000). A function for kinesin I in the posterior transport of oskar mRNA and Staufen protein. *Science* **289**, 2120-2122.

Brendza, R. P., Serbus, L. R., Saxton, W. M. and Duffy, J. B. (2002). Posterior localization of dynein and dorsal-ventral axis formation depend on kinesin in Drosophila oocytes. *Curr. Biol.* **12**, 1541-1545.

Cai, D., Hoppe, A. D., Swanson, J. A. and Verhey, K. J. (2007). Kinesin-1 structural organization and conformational changes revealed by FRET stoichiometry in live cells. *J. Cell Biol.* **176**, 51-63.

Cha, B. J., Serbus, L. R., Koppetsch, B. S. and Theurkauf, W. E. (2002). Kinesin I-dependent cortical exclusion restricts pole plasm to the oocyte posterior. *Nat. Cell Biol.* **4**, 592-598.

Coy, D. L., Hancock, W. O., Wagenbach, M. and Howard, J. (1999). Kinesin's tail domain is an inhibitory regulator of the motor domain. *Nat. Cell Biol.* **1**, 288-292.

Dietrich, K. A., Sindelar, C. V., Brewer, P. D., Downing, K. H., Cremo, C. R. and Rice, S. E. (2008). The kinesin-1 motor protein is regulated by a direct interaction of its head and tail. *Proc. Natl. Acad. Sci. USA* **105**, 8938-8943.

Duncan, J. E. and Warrior, R. (2002). The cytoplasmic dynein and kinesin motors have interdependent roles in patterning the Drosophila oocyte. *Curr. Biol.* **12**, 1982-1991.

Friedman, D. S. and Vale, R. D. (1999). Single-molecule analysis of kinesin motility reveals regulation by the cargo-binding tail domain. *Nat. Cell Biol.* **1**, 293-297.

Fuger, P., Behrends, L. B., Mertel, S., Sigrist, S. J. and Rasse, T. M. (2007). Live imaging of synapse development and measuring protein dynamics using two-color fluorescence recovery after photo-bleaching at Drosophila synapses. *Nat. Protoc.* **2**, 3285-3298.

Gho, M., McDonald, K., Ganetzky, B. and Saxton, W. M. (1992). Effects of kinesin mutations on neuronal functions. *Science* **258**, 313-316.

Gindhart, J. G. (2006). Towards an understanding of kinesin-1 dependent transport pathways through the study of protein-protein interactions. *Brief. Funct. Genomic. Proteomic.* **5**, 74-86.

Gross, S. P., Welte, M. A., Block, S. M. and Wieschaus, E. F. (2002). Coordination of opposite-polarity microtubule motors. *J. Cell Biol.* **156**, 715-724.

Gutzeit, H. O. and Koppa, R. (1982). Time-lapse film analysis of cytoplasmic streaming during late oogenesis of Drosophila. *J. Embryol. Exp. Morphol.* **67**, 101-111.

Hackney, D. D. and Stock, M. F. (2000). Kinesin's IAK tail domain inhibits initial microtubule-stimulated ADP release. *Nat. Cell Biol.* **2**, 257-260.

Hackney, D. D., Baek, N. and Snyder, A. C. (2009). Half-site inhibition of dimeric kinesin head domains by monomeric tail domains. *Biochemistry* **48**, 3448-3456.

Hirokawa, N. and Takemura, R. (2005). Molecular motors and mechanisms of directional transport in neurons. *Nat. Rev. Neurosci.* **6**, 201-214.

Hurd, D. D. and Saxton, W. M. (1996). Kinesin mutations cause motor neuron disease phenotypes by disrupting fast axonal transport in Drosophila. *Genetics* **144**, 1075-1085.

Imanishi, M., Endres, N. F., Gennerich, A. and Vale, R. D. (2006). Autoinhibition regulates the motility of the C. elegans intraflagellar transport motor OSM-3. *J. Cell Biol.* **174**, 931-937.

Januschke, J., Gervais, L., Dass, S., Kaltschmidt, J. A., Lopez-Schier, H., St Johnston, D., Brand, A. H., Roth, S. and Guichet, A. (2002). Polar transport in the Drosophila oocyte requires Dynein and Kinesin I cooperation. *Curr. Biol.* **12**, 1971-1981.

Lei, Y. and Warrior, R. (2000). The Drosophila Lissencephaly1 (DLis1) gene is required for nuclear migration. *Dev. Biol.* **226**, 57-72.

Ling, S. C., Fahrner, P. S., Greenough, W. T. and Gelfand, V. I. (2004). Transport of Drosophila fragile X mental retardation protein-containing ribonucleoprotein granules by kinesin-1 and cytoplasmic dynein. *Proc. Natl. Acad. Sci. USA* **101**, 17428-17433.

Liu, Z., Xie, T. and Steward, R. (1999). Lis1, the Drosophila homolog of a human lissencephaly disease gene, is required for germline cell division and oocyte differentiation. *Development* **126**, 4477-4488.

MacDougall, N., Clark, A., MacDougall, E. and Davis, I. (2003). Drosophila gurken (TGFalpha) mRNA localizes as particles that move within the oocyte in two dynein-dependent steps. *Dev. Cell* **4**, 307-319.

Martin, M., Iyadurai, S. J., Gassman, A., Gindhart, J. G., Jr, Hays, T. S. and Saxton, W. M. (1999). Cytoplasmic dynein, the dynactin complex, and kinesin are interdependent and essential for fast axonal transport. *Mol. Biol. Cell* **10**, 3717-3728.

Navone, F., Niclas, J., Hom-Booher, N., Sparks, L., Bernstein, H. D., McCaffrey, G. and Vale, R. D. (1992). Cloning and expression of a human kinesin heavy chain gene: interaction of the COOH-terminal domain with cytoplasmic microtubules in transfected CV-1 cells. *J. Cell Biol.* **117**, 1263-1275.

Ou, G., Blacque, O. E., Snow, J. J., Leroux, M. R. and Scholey, J. M. (2005). Functional coordination of intraflagellar transport motors. *Nature* **436**, 583-587.

Palacios, I. M. and St Johnston, D. (2002). Kinesin light chain-independent function of the Kinesin heavy chain in cytoplasmic streaming and posterior localisation in the Drosophila oocyte. *Development* **129**, 5473-5485.

Pilling, A. D., Horiuchi, D., Lively, C. M. and Saxton, W. M. (2006). Kinesin-1 and Dynein are the primary motors for fast transport of mitochondria in Drosophila motor axons. *Mol. Biol. Cell* **17**, 2057-2068.

Reid, E., Kloos, M., Ashley-Koch, A., Hughes, L., Bevan, S., Svenson, I. K., Graham, F. L., Gaskell, P. C., Dearlove, A., Pericak-Vance, M. A. et al. (2002). A kinesin heavy chain (KIF5A) mutation in hereditary spastic paraplegia (SPG10). *Am. J. Hum. Genet.* **71**, 1189-1194.

Rice, S. E. and Gelfand, V. I. (2006). Paradigm lost: milton connects kinesin heavy chain to miro on mitochondria. *J. Cell Biol.* **173**, 459-461.

Saxton, W. M., Hicks, J., Goldstein, L. S. and Raff, E. C. (1991). Kinesin heavy chain is essential for viability and neuromuscular functions in Drosophila, but mutants show no defects in mitosis. *Cell* **64**, 1093-1102.

Seeger, M. A. and Rice, S. E. (2010). Microtubule-associated protein-like binding of the kinesin-1 tail to microtubules. *J. Biol. Chem.* **285**, 8155-8162.

Seiler, S., Kirchner, J., Horn, C., Kallipolitou, A., Woehlke, G. and Schliwa, M. (2000). Cargo binding and regulatory sites in the tail of fungal conventional kinesin. *Nat. Cell Biol.* **2**, 333-338.

Serbus, L. R., Cha, B. J., Theurkauf W. E. and Saxton W. M. (2005). Dynein and the actin cytoskeleton control kinesin-driven streaming in Drosophila oocytes. *Development* **132**, 3743-3752.

Snow, J. J., Ou, G., Gunnarson, A. L., Walker, M. R., Zhou, H. M., Brust-Mascher, I. and Scholey, J. M. (2004). Two anterograde intraflagellar transport motors cooperate to build sensory cilia on C. elegans neurons. *Nat. Cell Biol.* **6**, 1109-1113.

Stock, M. F., Guerrero, J., Cobb, B., Eggers, C. T., Huang, T. G., Li, X. and Hackney, D. D. (1999). Formation of the compact conformer of kinesin requires a COOH-terminal heavy chain domain and inhibits microtubule-stimulated ATPase activity. *J. Biol. Chem.* **274**, 14617-14623.

Stone, M. C., Roegiers, F. and Rolls, M. M. (2008). Microtubules have opposite orientation in axons and dendrites of Drosophila neurons. *Mol. Biol. Cell* **19**, 4122-4129.

Theurkauf, W. E., Smiley, S., Wong, M. L. and Alberts, B. M. (1992). Reorganization of the cytoskeleton during Drosophila oogenesis: implications for axis specification and intercellular transport. *Development* **115**, 923-936.

Vale, R. D. and Milligan, R. A. (2000). The way things move: looking under the hood of molecular motor proteins. *Science* **288**, 88-95.

Vale, R. D., Reese, T. S. and Sheetz, M. P. (1985). Identification of a novel force-generating protein, kinesin, involved in microtubule-based motility. *Cell* **42**, 39-50.

Valentine, M. T. and Gilbert, S. P. (2007). To step or not to step? How biochemistry and mechanics influence processivity in Kinesin and Eg5. *Curr. Opin. Cell Biol.* **19**, 75-81.

Verhey, K. J. and Rapoport, T. A. (2001). Kinesin carries the signal. *Trends Biochem. Sci.* **26**, 545-550.

Welte, M. A. (2004). Bidirectional transport along microtubules. *Curr. Biol.* **14**, R525-R537.

Wong, Y. L., Dietrich, K. A., Naber, N., Cooke, R. and Rice, S. E. (2009). The Kinesin-1 tail conformationally restricts the nucleotide pocket. *Biophys. J.* **96**, 2799-2807.

Yonekura, H., Nomura, A., Ozawa, H., Tatsu, Y., Yumoto, N. and Uyeda, T. Q. (2006). Mechanism of tail-mediated inhibition of kinesin activities studied using synthetic peptides. *Biochem. Biophys. Res. Commun.* **343**, 420-427.

Zimyanin, V. L., Belaya, K., Pecreaux, J., Gilchrist, M. J., Clark, A., Davis, I. and St Johnston, D. (2008). In vivo imaging of oskar mRNA transport reveals the mechanism of posterior localization. *Cell* **134**, 843-853.